# Improved Genome Packaging Efficiency of AAV Vectors Using Rep Hybrids[#]

Mario Mietzsch[1], Courtnee Eddington[1], Ariana Jose[1], Jane Hsi[1], Paul Chipman[1], Tom Henley[2], Modassir Choudhry[2], Robert McKenna[1,*], and Mavis Agbandje-McKenna[1]

[1] Department of Biochemistry and Molecular Biology, Center for Structural Biology, McKnight Brain Institute, College of Medicine, University of Florida, Gainesville, FL 32610, USA
[2] Intima Bioscience, New York, USA

[#] Written in loving memory of Mavis Agbandje-McKenna

*Corresponding author: Robert McKenna, Department of Biochemistry and Molecular Biology,1600 SW Archer Road, P.O. Box 100245, Gainesville, FL 32610-0266, USA; Tel: +1 352 294 8395; e-mail: rmckenna@ufl.edu

Key words: Adeno-associated virus, Rep protein, capsid, genome packaging, cryo-electron microscopy, hybrid, empty and full capsids.

## *Abstract*

Recombinant Adeno-associated viruses (rAAVs) are one of the most commonly used vectors for a variety of gene therapy applications. In the last two decades research focused primarily on the characterization and isolation of new *cap* genes resulting in hundreds of natural and engineered AAV capsid variants while the *rep* gene, the other major AAV open reading frame, has been less studied. This is due to the fact that the *rep* gene from AAV serotype 2 (AAV2) enables the ssDNA packaging of recombinant genomes into most AAV serotype and engineered capsids. However, a major byproduct of all vector productions is empty AAV capsids, lacking the encapsidated vector genome, especially for non-AAV2 vectors. Despite the packaging process being considered the rate-limiting step for rAAV production, none of the *rep* genes from the other AAV serotypes have been characterized for their packaging efficiency. Thus, in this study AAV2 *rep* was replaced with the *rep* gene of a select number of AAV serotypes. However, this led to a lowering of capsid protein expression, relative to the standard AAV2-*rep* system. In further experiments the 3'end of the AAV2 *rep* gene was reintroduced to promote increased capsid expression and a series of chimeras between the different AAV Rep proteins were generated and characterized for their vector genome packaging ability. The utilization of these novel Rep hybrids increased the percentage of genome containing (full) capsids ~2-4-fold for all of the non-AAV2 serotypes tested. Thus, these Rep chimeras could revolutionize rAAV production.

## Importance

A major byproduct of all Adeno-associated virus (AAV) vector production systems are “empty” capsids, void of the desired therapeutic gene, and thus do not provide any curative benefit for the treatment of the targeted disease. In fact, empty capsids can potentially elicit additional immune responses *in vivo* gene therapies if not removed by additional purification steps. Thus, there is a need to increase the genome packaging efficiency and reduce the number of empty capsids from AAV biologics. The novel Rep hybrids from different AAV serotypes described in this study are capable of reducing the percentage of empty capsids in all tested AAV serotypes and improve overall yields of genome-containing AAV capsids at the same time. They can likely be integrated easily into existing AAV manufacturing protocols to optimize the production of the generated AAV gene therapy products.

## *Introduction*

Adeno-associated viruses (AAVs) are not associated with any pathogenic effects but are widely studied as they have been developed into one of the most promising gene therapy vectors for *in vivo* gene therapy for a wide variety of monogenetic diseases (1). To date, three AAV-vector-mediated gene therapies have gained approval for commercialization: Glybera, an AAV1 vector for the treatment of lipoprotein lipase deficiency (2); Luxturna, an AAV2 vector for the treatment of Leber's congenital amaurosis (3); and Zolgensma, an AAV9 vector for the treatment of spinal muscular atrophy type 1 (4). Common to all natural and engineered AAVs are their small, non-enveloped icosahedral capsids, of ~260 Å diameter, that contain a linear single-stranded DNA (ssDNA) genome (5). The wild-type AAVs have a genome size of approximately 4.7 kb (6). Both ends of the genome contain identical inverted terminal repeats (ITRs) of ~150 nucleotides (nts) that form T-shaped hairpin secondary structures and are important for genome replication and packaging (7). Between these ITRs, two open reading frames (ORFs) encode a series of replication (Rep) and virus proteins (VP) (8), as well as two smaller accessory proteins: the assembly activating protein (AAP) and the membrane-associated accessory protein (MAAP) (9, 10). For recombinant AAV vectors, these viral ORFs are replaced with an approximately similar-sized therapeutic gene of interest and only the flanking *cis*-active ITRs are retained to allow packaging of the recombinant genomes into the capsids. Nevertheless, the Rep and VP proteins are also needed for vector manufacturing but can be supplied in *trans* (11, 12).

The Rep proteins play critical roles in the viral replication cycle as well as for vector production (8). The four Rep proteins, Rep78, Rep68, Rep52, and Rep40, are situated in the same ORF and are translated from transcripts generated by the p5 and p19 promoter (13). The larger Rep78/68 proteins are extended by ~224 amino acids at their N-terminus in comparison to Rep52/40 and the C-terminus of Rep68/40 differs from those of Rep78/52 due to differential splicing (13). All Rep proteins share a central 305 amino acid stretch that contains a

helicase/ATPase domain (14) and nuclear localization signals (15). The N-terminus of Rep78/68 contains a DNA binding and endonuclease domain (16) whereas the C-terminus of Rep78/52 is suggested to contain a zinc finger domain (17). The large Rep proteins Rep78/68 are indispensable for genome replication and were shown to bind to a specific DNA sequence also present in the ITRs. The small Rep proteins Rep52/40 are essential for packaging of the genome into the capsids (18) formed by VP1, VP2, and VP3 that are encoded by the second ORF.

Similar to the Rep proteins the VPs are located in one ORF and share a common C-terminus. They are generated from transcripts of the p40 promoter by differential splicing and by the utilization of alternate start codons. VP1 is the largest capsid protein with approximately 735 amino acids and is encoded within the entire ORF. VP2 and VP3 are truncated at their N-termini relative to VP1 with ~598 and 533 amino acids, respectively. The VPs are expressed and incorporated into the capsid in an approximate ratio of 1:1:10 (VP1:VP2:VP3) (19). The capsid assembly is assisted by AAP which is encoded within the *cap* gene but situated in an alternate reading frame (9). Similarly, the second accessory protein MAAP is also encoded in an alternate reading frame within the *cap* gene and was suggested to have a role in capsid egress (10).

Packaging of the wild-type or recombinant vector genomes occurs in the nucleus into preformed “empty” VP capsids (20). Following replication of the genomes by the large Rep proteins, the generated ssDNA genomes are thought to be translocated into the capsid in 3' to 5' direction by the helicase/ATPase domain of the small Rep proteins (18). The translocation of the ssDNA into the preformed capsid is proposed to occur through a channel at the 5-fold symmetry axis of the AAV capsids (5). Since genome packaging is considered to be the rate limiting step a significant number of capsids go unpacked and remain empty. For AAV-mediated gene therapy these empty capsids are not desired as they do not provide any therapeutic benefit and may induce unwanted immune responses.

For the AAVs 13 primate AAV serotypes and numerous genotypes or engineered capsids have been described (21). The Rep and Capsid proteins of the AAV serotypes vary in amino acid sequence identity between ~52-99% (Table 1). This wide variety of available capsids is utilized in AAV-mediated gene therapy to package the transgene of choice into the capsid with the desired characteristics and tissue tropism. However, for the vast majority of manufactured AAV vectors the ITRs and *rep* gene of serotype 2 (AAV2) are utilized and only the *cap* gene is changed resulting in pseudotyped AAVs (22). While the Rep proteins of AAV2 are able to package vector genomes in all AAV serotype capsids their packaging efficiency is lower for some capsids compared to AAV2 (23). As a result, AAV vector preparations with non-AAV2 capsids contain a higher percentage of empty capsids.

Thus, in order to characterize the utilization of other *rep* genes in AAV vector productions, in this study the AAV2 *rep* gene was replaced with the *rep* gene of the same AAV serotype as the *cap* gene for a selection of different AAV serotypes. However, this substitution led to an overall lower VP expression for the analyzed AAV serotypes relative to the standard AAV2-*rep* system. Reverting the 3' end of the *rep* gene back to AAV2 as well as corrections in the DNA-binding domain of AAV8 Rep restored high capsid expression. In addition, a higher packaging efficiency of vector genomes was observed. In a series of chimeras, primarily the DNA binding and endonuclease domain of the AAV1 and AAV8 Rep was shown to be responsible for improved vector genome packaging for AAV1 and AAV8 vectors. These observations were confirmed by ELISA, qPCR, alkaline gel electrophoresis, and cryo-electron microscopy (cryo-EM) of affinity-purified AAV vector preparations and show that the new Rep hybrids can increase the number of genome-containing capsids 2 to 4-fold in the case of AAV1 and AAV8 when compared to AAV2-*rep* produced vectors. Furthermore, utilization of these hybrids for other AAVs such as AAV6, AAV9, and AAVrh.10 also show higher genome packaging efficiency. These observations indicate that the utilization of these Rep chimeras could revolutionize AAV vector production.

## *Results and Discussion*

*Substitution of the standard AAV2 rep gene*

In the last two decades a lot of research has focused on the characterization and isolation of new *cap* genes resulting in hundreds of natural and engineered AAV capsid variants (21, 24-27). At the same time, the *rep* gene has been largely ignored due to the fact that the Rep proteins of AAV2 also package recombinant vector genomes into almost all AAV serotypes or variant capsids. A major byproduct of all vector productions is empty AAV capsids, with even lower packaging efficiencies for non-AAV2 vectors (23). Compared to AAV2, the amino acid sequence identity of VP1 ranges from 82-88% for most AAV serotype capsids, with the exception of AAV4/5/11/12 (Table 1). For the foremost AAV serotypes, the amino acid sequence identity of Rep78 shows a similar range of 85-90% indicating a potential co-evolution of the Rep proteins with the capsid VPs, potentially due to optimal interaction of Rep proteins with the matched serotype capsids during genome packaging.

Thus, to understand the impact for the utilization of different AAV Rep proteins for AAV vector production, the AAV2 *rep* gene was replaced in the producer plasmids with the *rep* gene of the AAV serotype identical to the *cap* gene for the serotypes AAV1, 6, and 8 (Figure 1A). When the expression of the capsid proteins was analyzed all of new constructs demonstrated low to no VP expression (in the case of AAV8) compared to the standard AAV2 *rep* constructs (Figure 1B). The majority of AAV producer plasmids utilize AAV2 *rep* genes with the Rep78 start codon changed to an ACG, to lower the expression of the large Rep proteins in favor of the small Rep proteins (28). This strategy was shown to improve the overall AAV yield (29). Thus, ATG and ACG constructs for each producer plasmid were generated. While the Rep78 start codon had no significant effect on VP expression for any construct, the ACG start codon reduced Rep78/68 expression in all constructs as anticipated (Figure 1B) but in contrast to previous observations the overall yield of AAV vectors was not increased when using the ACG-Rep2 constructs (Figure 1C). In fact, the yield of AAV1 and AAV6 vectors using the AAV1 and

AAV6 *rep* constructs showed higher yields with the Rep78 having an ATG start codon. Another observation for the AAV1 and AAV6 *rep* constructs was their lower expression levels of spliced Rep proteins, Rep68 and Rep40, compared to the AAV2 *rep* constructs. The similar behavior of the AAV1 and 6 constructs was expected as their *rep* genes differ only in 36 nucleotides resulting in only four amino acid differences or 99% sequence identity (Table 1). This level of similarity between AAV1 and 6 is comparable to VP1 with only six amino acid differences between the AAV serotypes.

*Reintroduction of AAV2 sequences at the 3' end of AAV1 rep gene rescues VP expression*

The low expression of the capsid proteins prevents efficient AAV vector production. As the VPs are translated from transcripts generated from the p40 promoter, which is located in the 3' end of the *rep* gene, there was the possibility that the AAV1, 6, or 8 p40 promoter does not have same activity as the AAV2 p40 promoter. Alternatively, the observed reduced expression of Rep68/40 (Figure 1B) could indicate a disruption of mRNA splicing. The capsid proteins have been reported to be primarily translated from spliced p40 transcripts and mutations of the splice donor site resulted in a strong reduction of VP expression (30, 31). However, the splice donor consensus sequence of AAV1, 6, and 8 is identical to AAV2 (31). In order to test the first possibility, AAV p40-promoter luciferase reporter constructs were generated for AAV1, 2, and 8 and their luciferase expression analyzed (Figure 2A). Indeed, the AAV1 p40-promoter (AAV6 differs only by a single nucleotide) showed only about a quarter of the expression compared to AAV2. However, the AAV8 p40-promoter showed ~60% of the AAV2 p40-mediated expression (Figure 2A) even though VP expression was lower for the AAV8 construct compared to AAV1 (Figure 1B). Thus, there is the possibility of overlapping detrimental effects.

In order to rescue VP expression from the AAV1 *rep* constructs a series of swaps of the 3' end of the *rep* gene (or the C-terminus on protein level) for AAV1 and 2 were generated (Figure 2B). These constructs were analyzed for their expression of the Rep and capsid

proteins. As seen before the VP expression of the construct with the entire AAV1 rep (R1V1) was reduced and less Rep68/40 was observed compared to the standard AAV2 rep construct (R2V1) (Figure 2C). Substitution of the 3' end of AAV1 *rep* to AAV2 (R2c1V2) resulted only in a minor reduction of VP expression but showed less of Rep68/40. Vice versa, the introduction of 3' end of AAV2 *rep* in AAV1 increased VP expression and showed higher expression of the spliced Rep68/40 proteins (Figure 2C). To further narrow down the region responsible for these effects the 3' end of the rep gene was divided into two parts. The first (y) region contains the p40-pomoter and the splice donor site whereas the second (z) region comprises the sequence encoding the zinc-finger domain (Figure 2B). Swapping the y region to the respective sequences of the other AAV serotype resulted in little to no differences of the VP and Rep expression when compared to the constructs with the wild-type AAV1 or AAV2 rep gene (Figure 2C). This observation was surprising given the differential p40-promoter activities (Figure 2A). In contrast, swapping the zinc-finger domain sequences to the respective other AAV serotype resulted in significant differences of VP and Rep expression. The R2z1V1 construct showed a reduction of VP expression and a lower expression of Rep68/52 compared to Rep78/52 (Figure 2C). Vice versa, R1z2V1 showed an increase of VP expression and an approximately equal expression of Rep68/52 to Rep78/52 unlike the R1V1 construct. Thus, it is possible that these observations are linked, particularly since the VPs are translated from spliced p40 transcripts and mutations of the splice sites result in a strong reduction of VP expression (30, 31). In absence of nucleotide differences of the splice site in the AAV1 *rep* gene, the z-region, which comprises the majority of the intron sequence, has to be responsible for the inefficient splicing. Further research will be needed to determine whether the splice reduction is caused by the zinc-finger domain of the Rep proteins or by the differences of the DNA sequences. However, for this study the rescue of VP expression was achieved, and all subsequent variants contained the 3'end of the AAV2 *rep* gene.

*Rescue of AAV8 VP expression by correction of the AAV8 Rep DNA binding domain.*

The substitution of the 3'end of the *rep* gene to the sequences of AAV2 rescued AAV1 VP expression as shown above (Figure 2C) and AAV6 VP expression (data not shown). Thus, the same strategy was pursued in the case of AAV8 vector production using the AAV8 *rep* gene (Figure 3A). However, unlike the AAV1 and AAV6 constructs, no significant AAV8 VP expression was observed with the R8c2V8 construct (Figure 3B), comparable to the R8V8 construct as seen before (Figure 1B). Furthermore, the inability to express VP proteins was not just restricted to AAV8, as AAV1 and AAV6 VP expression is also inhibited when the AAV8 rep gene was utilized (data not shown). Vice-versa, AAV8 VP expression can be restored when using the AAV1 *rep* gene with the AAV2 3' end (R1c2V8) to a similar level compared to the standard AAV2 *rep* system (Figure 3B). This observation was surprising given the 95% amino acid sequence identity between AAV1 Rep and AAV8 Rep (Table 1). In order to identify the region of the AAV8 *rep* gene responsible for this phenotype *rep* was sectioned into three additional parts (n, d, and h) and substituted to the corresponding AAV1 sequences (Figure 3A). Significant AAV8 VP expression was only achieved when the d-region was substituted for the AAV1 sequences (R8d1c2V8, Figure 3B) which is equivalent to the sequence encoding the DNA-binding domain. Further experiments showed that the lack of efficient AAV8 VP expression with the AAV8 rep gene can also be rescued by the addition of an AAV1 Rep expression construct (p5-Rep1) *in trans* (Figure 3C). Conversely, an AAV8 Rep expression construct (p5-Rep8) does not repress AAV8 VP expression when using the standard AAV2 Rep system or enhance VP expression in the R8c2V8 construct. These observations point to a defect of the AAV8 Rep protein, that is associated with the DNA binding domain. A sequence analysis of AAV8 to AAV1 Rep (and other AAV serotypes) in the affected region revealed two highly variable regions termed VR-A (residues 117-126, with 8 amino acid substitutions and 1 insertion) and VR-B (residues 137-143, with 5 amino acid substitutions and 1 insertion) (Figure

3D). However, when the sequences were analyzed on DNA sequence level only two nucleotide exchanges and 3 insertions were found for VR-A and one nucleotide exchange and 3 insertions for VR-B, respectively. The fact that the individual nucleotide insertions of AAV8 are spread out results in a shift of the reading frame relative to AAV1 and causes the high amino acid variability despite little differences at the DNA level. Since both VRs contain 3 nucleotide insertions the ribosomes shift back into the original reading frame during translation (Figure 3D). The occurrence of the 3 spaced-out nucleotide insertions is unlikely to happen naturally as they would need to be introduced simultaneously. Otherwise, the individual insertions would shift the reading frame and truncate the Rep proteins significantly. Thus, it is more likely that these insertions represent sequencing errors of the deposited AAV8 *rep* gene sequence. Therefore, the nucleotide sequences of VR-A and VR-B were corrected by removing the nucleotide insertions relative to AAV1 which resulted in a highly similar amino acid sequences with only a single amino acid substitution in VR-A and the identical amino acid sequence in VR-B (Figure 3D). Following transfection of these constructs the AAV8 VP expression was analyzed. While the correction of VR-A alone did not improve VP expression, the construct with the corrected VR-B showed significant VP expression (Figure 3E). This expression was further enhanced when both corrected regions were combined resulting in a similar VP expression compared to the R8d1c2V8 construct. The rescue of AAV8 VP expression can be explained based on a previously determined X-ray crystallography structure of AAV2 Rep bound to its binding element within the AAVS1 sequence (32). A model generated for the uncorrected AAV8 Rep protein based on the AAV2 Rep structure placed VR-A distance from, but VR-B directly in the major groove of the bound DNA (Figure 3F). While VR-A does not directly bind to the DNA, it could stabilize the binding of VR-B to the DNA and thus, further enhance VP expression. As the Rep proteins have been described as an activator of AAV transcription (33) it is possible that the defective AAV8 Rep proteins are unable to transactivate the p40 promoter (34) needed for efficient VP expression.

*AAV1/2 Rep hybrids can enhance vector genome packaging efficiency into AAV1 capsids.*

Initial analyses of lysates showed that vector genome titers were comparable to the standard AAV2 rep system (R2V1) when the ATG-R1V1 construct was used despite displaying lower VP expression (Figure 4A). Following the rescue of the VP expression with ATG-R1c2V1, the genome titer was higher than R2V1 but at a similar VP expression level. However, this enhancement was only observed for the ATG start codon constructs while the ACG constructs showed very low genome titers (Figure 4A).

Thus, the genome packaging efficiency of the Rep hybrids into AAV1 capsids was further investigated. For this purpose, the *rep* genes of AAV1 and AAV2 were divided into 3 additional regions (n, d, and h) similar as described for AAV8 above to identify which region provides a potential benefit for genome packaging (Figure 4B). For these regions eight possible permutations between AAV1 and AAV2 were generated (R2, R2n1, R2d1, R2h1, R1c2, R1nc2, R1dc2, and R1hc2) and utilized for AAV1 vector production. As the packaging efficiency was expected to vary slightly between different vector preparations three independent vector preparations for each Rep variant were produced. The individual AAV1 vector preparations were purified also independently by AVB affinity chromatography that indiscriminately binds empty and full capsids (35). Subsequently, each of the AAV1 vector preparations were analyzed by cryo-electron microscopy (cryo-EM) and the percentage of full capsids determined (Figure 4C). For the standard AAV2 Rep production system (R2V1) the percentage of full capsids in the three vector preparations ranged from ~10-20% with a mean average of 15% (Table 2). In contrast, for AAV1 Rep with the AAV2 C-terminus (R1c2V1) the percentage of full capsids in the three vector preparations is approximately doubled and ranged from 25-37% with a mean average of 32%. Swaps of the N-termini based on these constructs to the corresponding other AAV serotype was detrimental to both constructs. While the AAV1 N-terminus in AAV2 Rep (R2n1V1) resulted in a vast majority of empty capsids (% full: 1-2%, average: ~1%), the AAV2

294 N-terminus in AAV1 (R1nc2V1) reduced the percentage of full capsids to 9-11% with a mean
295 average of 10% (Figure 4C, Table 2). Similarly, the AAV2 DNA-binding domain inserted into
296 AAV1 Rep (R1dc2V1) also resulted in largely empty capsids (% full: 1-2%, average: ~2%).
297 These results could indicate that the AAV2 DNA binding domain is not compatible with the
298 AAV1 N-terminus which are expressed by the R2n1V1 and R1dc2V1 constructs. Vice versa, the
299 AAV1 DNA-binding domain is supported in AAV2 Rep and slightly enhanced packaging
300 efficiency (% full: 15-24%, average: ~20%). Swapping the AAV1 helicase domain into AAV2
301 (R2h1V1) did not affect the packaging efficiency significantly (% full: 9-17%, average: ~12%)
302 compared to R2V1. Lastly, the Rep hybrid with the best overall packaging efficiency contained
303 the AAV2 helicase within AAV1 Rep (R1hc2V1) with a percentage of full capsids in the four
304 vector preparations ranging from 24-48% with a mean average of 38% (Figure 4D, Table 2).
305 The approximate full-empty ratios for the different Rep hybrids were also confirmed by qPCR
306 when compared to the capsid titer determined by ELISA (data not shown). The packaged
307 genomes were also visualized by performing an alkaline gel electrophoresis loading equal
308 amounts of capsids (Figure 4D). Thus, vector preparations with a higher percentage of full
309 capsids will appear brighter such as for R1hc2V1 whereas no bands are seen for largely empty
310 capsids (R2n1V1 and R1dc2V1). Regardless of the utilized Rep hybrid during vector production,
311 no significant differences of the transduction efficiency of the purified AAV vectors were
312 observed (Figure 4E). This was expected as the Rep proteins are not part of the final purified
313 AAV vector preparations.
314
315 *The Rep hybrids also enhance vector genome packaging efficiency for other AAV serotypes.*
316 A similar screen for the genome packaging efficiency, as done for AAV1 (Figure 4A),
317 was conducted for AAV6 utilizing AAV6 hybrids with the AAV2 C-terminus. However, the AAV1
318 and AAV8 *rep* hybrids cloned upstream of the AAV6 *cap* gene appeared to exceed the
319 packaging efficiency over the AAV6 Rep hybrids (data not shown). Thus, the AAV1 and AAV8

Rep hybrids were utilized for AAV6 production and compared to the standard AAV2 Rep system (Figure 5A). Similar to AAV1 the three independent AAV6 vector preparations were purified by AVB-affinity chromatography and the percentage of full capsids determined by cryo-EM imaging. For the standard AAV2 Rep system (R2V6) the percentage of full capsids ranged from 12-20% (average 17%) (Table 3). In contrast, the percentage of full capsids is increased for each of the other tested Rep hybrids ranging from 20-39% (average 28%) for R2d1V6, 37-46% (average 43%) for R1hc2V6, and 32-38% (average 36%) for R8d1c2V6 (Figure 5A, Table 3). Due to the high sequence similarity of the AAV1 and AAV6 capsids (36) it was not surprising that the Rep hybrids improved packaging efficiency similarly.

For AAV8 vectors produced with AAV2 *rep* and the percentage of full capsids ranged from 18-23% (average 20%) (Figure 5B, Table 3). The utilization of the Rep hybrids that also rescued AAV8 VP expression (Figure 3) improved the percentage of genome-containing capsids to 27-41% (average 33%) for R1c2V8, 28-47% (average 36%) for R8d1c2V8, and 30-62% (average 43%) for the corrected R8c2V8. Following the correction of the AAV8 DNA binding domain (Figure 3D) the resulting Rep protein of the R8c2V8 construct varies only in two amino acids from the R8d1c2 Rep hybrid. Thus, a similar level of enhancement of genome packaging efficiency was expected.

For AAV9 and AAVrh.10 the *rep* genes or Rep protein sequences have not been isolated or deposited (21). Alternatively, the most promising Rep hybrids for AAV1, AAV6, and AAV8 were cloned upstream of the AAV9 or AAVrh.10 *cap* gene and the yield of the constructs by qPCR compared to the VP expression intensity by Western-blot (data not shown). For both AAVs the R8d1c2 Rep hybrid came ahead of the standard AAV2 Rep and three independent AAV preparations were generated with either Rep variant as with the previous AAV serotypes for detailed analysis. For AAV9 the percentage of full capsids ranged from 14-22% (average: 18%) with R2V9 whereas genome-containing capsids were increased to 29-36% (average: 32%) with R8d1c2V9 (Figure 5C). For AAVrh.10 the results were similar with 11-28% (average

346 17%) full capsids with R2Vrh.10 and 27-34% (average 31%) full capsids with R8d1c2Vrh.10
347 (Figure 5D, Table 3).

348 These results indicate that the new Rep hybrids may improve packaging regardless of
349 which capsids are utilized as the amino acid sequence identity of these capsids vary from 82-
350 99% (Table 1). In order to confirm this conclusion, the effects of the Rep hybrids were also
351 analyzed on AAV2 vector production. As expected, the overall yield of capsids with the different
352 Rep hybrids were comparable (Figure 6A) but the vector genome cassettes were packaged
353 equally (Figure 6B). As previously mentioned, packaging of vector genomes into AAV2 capsids
354 is generally more efficient (23). This was also observed using cryo-EM imaging with the R2V2
355 construct generating ~47% of full capsids (Figure 6C). In contrast, the percentage of full capsids
356 for the other AAV serotypes ranged from 12-20% when the AAV2 *rep* gene was used (Figure
357 4C, Figure 5). With the different Rep hybrids, the percentage of full AAV2 capsids ranged
358 between 32 – 65% (Figure 6C) which corresponds to a 0.7-1.4-fold decrease or increase
359 relative to the wtAAV2 Rep construct, respectively. As the portion of genome-containing capsids
360 was high for AAV2 to start with, a further improvement of packaging was not expected. On the
361 other hand, utilizing the Rep hybrids such as R1c2 or R8d1c2 for AAV2 vector production the
362 percentage of full AAV2 capsids did not drop significantly either. This questioned the initial
363 hypothesis that the Rep proteins of an AAV serotype might be adapted to its own capsid. Thus,
364 there has to be an alternative explanation for the higher percentage of full capsids when using
365 these Rep hybrids. The Rep hybrids that allowed the best packaging efficiency contained the
366 ~240 N-terminal amino acids of either AAV1 or AAV8 Rep78/68 which contains the DNA-
367 binding and endonuclease domain of the Rep proteins (16). This region is indispensable for
368 genome replication (18, 37, 38). Thus, it is possible that the Rep hybrids replicate the vector
369 genomes to higher copy numbers prior to their packaging. However, the copy number of vector
370 genomes determined by qPCR after lysis of transfected cells without DNase treatment showed
371 similar level of replicated genomes for all Rep variants (data not shown). The small Rep proteins

(Rep52/40) have been suggested to be responsible for the encapsidation of the genomes into the capsids (18). However, the small Rep proteins are largely identical between Rep2 and the R1hc2 variant (Figure 4D) except for a single amino acid substitution (K234R). Thus, it is likely that the large Rep proteins are also involved in the encapsidation process with the Rep hybrids improving genome packaging by a currently unknown mechanism.

*Conclusions.*

The vast majority of AAV production systems utilize AAV2 *rep* for vector manufacturing. The few exceptions reported previously include the utilization of the *rep* gene of AAV3 (39) and AAV4 (22) for production. In both cases the vector yield was described to be higher, but no further investigation was conducted. In this study the *rep* genes of different AAV serotypes were analyzed and while they were not directly usable “as is”, they were modified to generate hybrids supporting high capsid expression and improved packaging efficiency. The fact that the Rep hybrids enhanced packaging efficiency across multiple, widely used AAV serotypes in gene therapy trials indicates that they can be possibly used for almost all AAV capsids to improve overall vector yield and increase of the percentage of genome-containing capsids. As the *rep* gene is often provided *in trans* for most AAV production system the new hybrid *rep* genes can easily replace the AAV2 *rep* constructs. Furthermore, during AAV vector purification the Rep proteins are removed, making the final product indistinguishable to the AAV2 *rep* system except for the higher content of genome-containing capsids. While the exact mechanism of the enhancement of packaging remains unclear further research on the Rep proteins is needed in general. It will be also interesting to see if the Rep hybrids also improve packaging in insect cells for large scale AAV production setups that often suffer from high empty-to-full capsid ratios (40). Empty capsids are generally not desired in AAV vector preparations as they do not provide any curative benefit for the treatment of the targeted disease and can reduce overall transduction efficiencies (41). Some purification protocols do not actively remove empty capsid

398 which could be problematic when administered to a patient with a given genome-containing
399 vector dose as the empty particle titer can be 5 to 10-fold higher. These empty capsids can then
400 potentially elicit additional immune responses *in vivo* gene therapies.

## *Materials and Methods*

*Plasmids and cloning*

The *rep* genes of AAV1, AAV6, and AAV8 were synthesized by GenArt (Thermo Fisher) based on the deposited AAV serotype genomes; accession numbers: AF063497 (AAV1), AF043303 (AAV2), and AF513852 (AAV8). These rep genes were inserted into plasmids containing the AAV2 *rep* gene and either the AAV1, 6, or 8 *cap* gene (R2V1, R2V6, or R2V8) by replacing the AAV2 *rep* gene to generate R1V1, R6V6, or R8V8, respectively. Site-directed mutagenesis was utilized by as previously described (42) to mutate the Rep78 start codon or to correct the AAV8 *rep* gene. In order to generate Rep hybrid proteins, the *rep* gene was subdivided into four regions and cloned using restriction sites that are conserved in equivalent positions of the AAV1, 2, 6, and 8 rep genes. Briefly, the N-terminal region (n) extends to *Nco*I (nt position 305 of the AAV1 *rep* gene, amino acid position 102 of AAV1 Rep), the DNA-binding domain (d) to *BamH*I (nt position 725, amino acid position 242), the helicase domain (h) to *Sal*I (nt position 1108, amino acid position 370) and the C-terminal region consists all the sequences past *Sal*I. In absence of usable restrictions site Gibson assembly was performed using the NEB Gibson assembly master mix according to the manufacturer instructions to further subdivide the C-terminal region at nt position 1590, amino acid position 530 (AAV1 numbering), termed y and z region. To determine the p40 promoter activity the nts 1442-1878 (AAV1), nts 1428-1887 (AAV2), and nts 1340-1776 (AAV8) from the accession numbers listed above were cloned upstream of a luciferase gene.

Cell culture

HEK293 cells were maintained in Dulbecco's Modified Eagle Medium (DMEM) supplemented with 10% heat-inactivated fetal calf serum and 100 U of penicillin/ml and 100 µg of streptomycin at 37°C in 5% $CO_2$.

427 *AAV production and purification*

428 Recombinant AAV vectors, with a packaged luciferase gene, were produced by triple
429 transfection of HEK293 cells, utilizing pTR-UF3-Luciferase, pHelper (Stratagene), and a *rep-cap*
430 plasmid containing either the wild-type or hybrid *rep* genes. The transfected cells were
431 harvested 72 h post transfection as previously described (42). The cleared lysates containing
432 AAV capsids were purified by AVB Sepharose (Thermo Fisher) in the case of AAV1, 2, and 6
433 and by POROS CaptureSelect™ AAV8 (Thermo Fisher) affinity chromatography as previously
434 described (35).

435

436 SDS-PAGE and Western-blot analysis

437 The purity of the AAV preparations were confirmed by sodium dodecyl sulfate
438 polyacrylamide gel electrophoresis (SDS-PAGE). For this purpose, the samples were incubated
439 with 6× Laemmle Sample Buffer (Bio-Rad) with 10% β-mercaptoethanol and boiled for 5 min at
440 100°C. The denatured proteins were applied to a 10% polyacrylamide gel and ran at 120 V. The
441 gel was washed three times with distilled water (diH2O) and stained with GelCode Blue Protein
442 Safe stain (Invitrogen). In order to confirm and evaluate Rep and Cap expression from the new
443 Rep hybrid plasmids Western-blot analyses were performed. For this purpose, the proteins were
444 transferred to a nitrocellulose membrane following SDS-PAGE by electroblotting. The
445 membrane was blocked in 6% milk in 1xPBS and probed with hybridoma supernatants
446 containing MAb B1, detecting VP1, VP2, and VP3, (43) or MAb 1F, detecting Rep78, Rep68,
447 Rep52, and Rep40 (29). Following the incubation with a secondary antibody with a linked horse
448 radish peroxidase the proteins were visualized by applying Immobilon™ Chemiluminescent
449 Substrate (Millipore) and detection on an X-ray film.

450

451 *Quantification of AAV vectors*.

Aliquots from the AAV vector preparations were digested with Proteinase K to release the AAV vector genomes from the capsids. To this end, the samples were incubated in buffer containing 10 mM Tris pH 8, 10 mM EDTA, 1% SDS for 2 h at 56°C. The released DNA was purified utilizing the PureLink PCR Purification Kit (Thermo Fisher). The copy number of vector genome DNAs were determined by quantitative PCR using iQ™ SYBR® Green Supermix (BioRad, Hercules, CA). Primers specific for the luciferase gene of the vector genome were used (Forward primer 5'-GCAAAACGCTTCCATCTTCC-3' and reverse primer 5'-AGATCCACAACCTTCGCTTC -3').

*AAV capsid ELISA*.

For the quantification of the physical capsid titer AAV Titration ELISA (Progen) were utilized. All the steps were done according to the protocol provided by the manufacturer in triplicate. The colorimetric assay was analyzed by a Synergy HT plate reader (BioTek).

*Alkaline gel electrophoresis*.

For the alkaline gel electrophoresis, a 0.8 % agarose gel in 1xTAE buffer (40 mM Tris, 20 mM acetic acid, and 1 mM EDTA) was utilized. Following solidification, the gel was equilibrated in 1x denaturing buffer (0.5 M NaOH, 50 mM EDTA) for 4 h. Prior to the loading, the samples were mixed with denaturing loading dye (final concentration: 1x Ficoll loading buffer, 1x denaturing buffer, 10% SDS). The agarose gel was run at low voltage overnight at 4°C. After the run the gel was washed and neutralized in 1xTAE for 30 min and subsequently stained in a 0.02% SyBr-Gold solution in 1xTAE. The gel was imaged under UV light using a BioRad GelDoc system.

Analysis of transduction efficiency and promoter activity

Purified AAV vectors with a packaged luciferase expression cassette were used to infect HEK-293 cells at a $10^5$ MOI (multiplicity of infection). After 48 h, cells were lysed and luciferase activity assayed using a luciferase assay kit (Promega) as described in the manufacturer's protocol. Luminescence was measured on a Synergy HT plate reader (BioTek). In order to determine the p40 promoter activity in HEK293 cells the AAV-p40-luciferase constructs were transfected and the cells incubated for 24 hours. The subsequent steps were performed identically as described above for the analysis of transduction efficiency.

*Cryo-Electron microscopy imaging*

For each of the purified AAV capsids, 3.5 µL was applied to a glow-discharged Quantifoil copper grid with 2 nm continuous carbon support over holes (Quantifoil R 2/4 400 mesh), blotted, and vitrified using a Vitrobot Mark 4 (FEI) at 95% humidity and 4°C. Images were collected using an FEI Tecnai G2 F20-TWIN microscope (FEI) operated under low-dose conditions (200 kV, ~20$e^-$/Å$^2$) on a GatanUltraScan 4000 CCD camera (Gatan). The number of empty and full capsids in these images were counted manually.

**Acknowledgments**

The authors thank the UF-ICBR Electron microscopy core for access to electron microscopes utilized for cryo-electron micrograph screening.

**Conflicts of Interest**

The University of Florida Research Foundation has filed and licensed patent applications based on the findings described herein.

## *Figure Legends*

**Figure 1:** Substitution of the AAV2 *rep* gene. **A)** Overview of the utilized *rep-cap* constructs. AAV genes derived from AAV1 are colored in purple, AAV2 in blue, AAV6 in pink, and AAV8 in green. The construct name indicates the utilized Rep78 start codon (ATG or ACG) as well as the origin of the *rep* (R) and *cap* (V) gene (e.g. R2V1: *rep* gene from AAV2 and *cap* gene from AAV1). **B)** Analysis of Rep and VP expression by Western-blot following transfection of the constructs in HEK293 cells. Top blots were probed with MAb B1 and lower blots with MAb 1F. The individual VPs and Rep proteins are indicated.

**Figure 2:** Role of the 3' end of the rep gene in VP expression. **A)** Analysis of the p40 promoter activity from AAV1, AAV2, and AAV8 driving luciferase expression in HEK293 cells 24 h post transfection. The nucleotide positions of the fragments used are shown below the constructs based on the accession numbers: AF063497 (AAV1), AF043303 (AAV2), and AF513852 (AAV8). RLU: relative light units. **B)** Schematic depiction of the Rep protein with its main domains. The approximate position of the p40 promoter in the *rep* gene is indicated. Below the p5 and p19 transcripts are shown with the translated regions for Rep78, Rep68, Rep52, and Rep40. The C-terminal (c) ~250 aa has been subdivided into a N-terminal y-region and C-terminal z-region. The construct generated with all permutations between AAV1 and AAV2 involving these regions are depicted. Rep gene fragments derived from AAV1 are colored in purple and AAV2 in blue. **C)** Western-blot analysis to determine Rep and VP expression of the constructs. Top blots were probed with MAb B1 and lower blots with MAb 1F. The individual VPs and Rep proteins are indicated.

**Figure 3:** Rescuing VP expression utilizing the AAV8 *rep* gene. **A)** Schematic depiction of the Rep protein with its main domains. The approximate position of the p40 promoter in the *rep* gene is indicated. Below the p5 and p19 transcripts are shown with the translated regions for

Rep78, Rep68, Rep52, and Rep40. Rep has been subdivided into a N-terminal domain (n), the DNA-binding domain (d), the helicase domain (h), and a C-terminal domain (c). The generated constructs containing different domains from AAV1, AAV2, and AAV8 are depicted below. Rep gene fragments derived from AAV1 are colored in purple, AAV2 in blue, and AAV8 in green. **B)** Western-blot analysis to determine Rep and VP expression of the constructs shown in A. Top blots were probed with MAb B1 and lower blots with MAb 1F. The individual VPs and Rep proteins are indicated. **C)** Analysis as in (B) in presence or absence of co-transfected Rep constructs. **D)** Amino acid sequence alignment of AAV1 and AAV8 in the DNA-binding domain (aa110 to aa150). Identical residues are highlighted in yellow and amino acid with similar properties in green. The two regions of significant amino acid difference termed VR-A and VR-B are indicated. Below an analysis of these regions are shown at nucleotide level with the encoded amino acids shown. Deletions in AAV1 relative to AAV8 are highlighted in red. The insertions in AAV8 potentially result in shifts to an alternative reading frame. Removal of these insertion (AAV8*) result in a similar amino acid sequence to AAV1. **E)** Analysis as in (B) utilizing the AAV8 Rep variants with the removed insertions. The intensity of the VP bands was quantified using ImageJ and normalized to R8d1c2V8. **F)** Structural analysis of the DNA-binding site for AAV2-Rep (blue) and a superposed AAV8-Rep model (green) to AAVS1 dsDNA. The position of VR-A and VR-B is indicated.

**Figure 4:** AAV1/2 Rep hybrids improve AAV1 genome packaging efficiency. **A)** Analysis of VP expression by Western-blot and the AAV1 vector yield by qPCR following transfection of the constructs in HEK293 cells. The Western blot was probed with MAb B1. The individual VPs and Rep proteins are indicated. **B)** Schematic depiction of the Rep protein with its main domains. The approximate position of the p40 promoter in the *rep* gene is indicated. Below the p5 and p19 transcripts are shown with the translated regions for Rep78, Rep68, Rep52, and Rep40. Rep has been subdivided into a N-terminal domain (n), the DNA-binding domain (d), the

552 helicase domain (h), and a C-terminal domain (c). The generated constructs containing different
553 domains from AAV1 and AAV2 are depicted below. Rep gene fragments derived from AAV1 are
554 colored in purple and AAV2 in blue. **C)** Analysis of the AVB-purified AAV1 vector preparations.
555 Sections of SDS-PAGEs containing VP1, VP2, and VP3 and representative example cryo-EM
556 micrographs are shown for each Rep hybrid. White arrows point to empty capsids (light
557 appearance) and black arrows to full capsids (dark appearance). The determined percentage of
558 full capsids of at least three independently produced and purified AAV1 vector preparations are
559 displayed with the total particle count of all micrographs collected for the individual sample.
560 Scale bar (shown in R2V1 micrograph): 50 nm. **D)** Alkaline gel electrophoresis of the AAV1
561 vector preparations. Capsid amount loaded is the same for all samples based on the ELISA
562 titer. The size of the packaged vector genome (vg) is ~3.9 kb. **E)** Analysis of the transduction
563 efficiency of the AAV1 vectors produced with different Rep hybrids in HEK 293 cells.
564
565 **Figure 5:** The Rep hybrids also enhance packaging efficiency for other AAV serotypes. **A)**
566 Analysis of the AVB-purified AAV6 vector preparations. Sections of SDS-PAGEs containing
567 VP1, VP2, and VP3 and representative example cryo-EM micrographs are shown for each Rep
568 variant. White arrows point to empty capsids (light appearance) and black arrows to full capsids
569 (dark appearance). The determined percentage of full capsids of three independently produced
570 and purified AAV6 vector preparations are displayed with the total particle count of all
571 micrographs collected for the individual sample. Scale bar (shown in R2V6 micrograph): 50 nm.
572 **B)** Analysis as in (A) for AAV8-Capture select affinity ligand purified AAV8 vectors. **C)** Analysis
573 as in (A) for AAV9-Capture select affinity ligand purified AAV9 vectors. **D)** Analysis as in (A) for
574 AVB-purified AAVrh.10 vectors.
575
576 **Figure 6:** The effect of the Rep hybrids on genome encapsidation of AAV2. **A)** SDS-PAGE of
577 the AVB-purified AAV2 vector preparations produced with different Rep variants. VP1, VP2, and

578 VP3 are indicated. **B)** Alkaline gel electrophoresis of the AAV2 vector preparations. Capsid
579 amount loaded is the same for all samples. The size of the packaged vector genome (vg) is
580 ~3.9 kb. **C)** Representative example cryo-EM micrographs are shown for each Rep variant.
581 White arrows point to empty capsids (light appearance) and black arrows to full capsids (dark
582 appearance). The determined percentage of full capsids of the vector preparations are
583 displayed with the total particle count of all micrographs collected for the individual sample.
584 Scale bar (shown in R2V2 micrograph): 50 nm.

585 **Table 1:** Comparison of the VP1 and Rep78 amino acid sequence identity of the AAV serotypes

| | AAV1 | AAV2 | AAV3 | AAV4 | AAV5 | AAV6 | AAV7 | AAV8 | AAV9 | AAV10 | AAV11 | AAV12 | AAV13 |
|---|---|---|---|---|---|---|---|---|---|---|---|---|---|
| **AAV1** | | 83 | 87 | 63 | 58 | 99 | 85 | 84 | 82 | 85 | 66 | 60 | 87 |
| **AAV2** | 87 | | 88 | 60 | 57 | 83 | 82 | 83 | 82 | 84 | 63 | 60 | 88 |
| **AAV3** | 89 | 89 | | 63 | 58 | 87 | 85 | 86 | 84 | 86 | 65 | 61 | 94 |
| **AAV4** | 90 | 90 | 93 | | 53 | 63 | 63 | 63 | 62 | 63 | 81 | 78 | 65 |
| **AAV5** | 58 | 58 | 58 | 58 | | 58 | 58 | 58 | 57 | 57 | 53 | 52 | 58 |
| **AAV6** | 99 | 87 | 89 | 89 | 58 | | 85 | 84 | 82 | 85 | 66 | 60 | 87 |
| **AAV7** | 98 | 88 | 90 | 90 | 58 | 98 | | 88 | 82 | 88 | 67 | 62 | 85 |
| **AAV8** | 95 | 85 | 87 | 88 | 57 | 95 | 96 | | 85 | 93 | 65 | 62 | 85 |
| **AAV9** | N/A | N/A | N/A | N/A | N/A | N/A | N/A | N/A | | 86 | 64 | 60 | 84 |
| **AAV10** | 97 | 88 | 89 | 90 | 58 | 97 | 97 | 95 | N/A | | 66 | 61 | 86 |
| **AAV11** | 97 | 88 | 89 | 89 | 58 | 97 | 97 | 95 | N/A | 100 | | 84 | 65 |
| **AAV12** | 87 | 88 | 89 | 88 | 58 | 87 | 88 | 85 | N/A | 88 | 88 | | 60 |
| **AAV13** | 89 | 90 | 93 | 99 | 58 | 89 | 90 | 88 | N/A | 89 | 89 | 88 | |

**VP1 amino acid sequence identity [%]**

**Rep78 amino acid sequence identity [%]**

586

587 **Table 2:** Summary of the quantification of the full capsids for AAV1

| AAV serotype (capsid) | Utilized Rep variant | biological replicate | percentage "full" capsids | mean |
|---|---|---|---|---|
| AAV1 | R2 | I | 10% | 15% |
| | | II | 17% | |
| | | III | 19% | |
| | R2n1 | I | 1% | 1% |
| | | II | 2% | |
| | | III | 1% | |
| | R2d1 | I | 24% | 20% |
| | | II | 15% | |
| | | III | 21% | |
| | R2h1 | I | 9% | 12% |
| | | II | 17% | |
| | | III | 9% | |
| | R1c2 | I | 37% | 32% |
| | | II | 35% | |
| | | III | 25% | |
| | R1nc2 | I | 9% | 10% |
| | | II | 11% | |
| | | III | 10% | |
| | R1dc2 | I | 2% | 2% |
| | | II | 1% | |
| | | III | 2% | |
| | R1hc2 | I | 44% | 38% |
| | | II | 48% | |
| | | III | 35% | |
| | | IV | 24% | |

588

589 **Table 3:** Summary of the quantification of the full capsids for AAV6, 8, 9, and rh.10

| AAV serotype (capsid) | Utilized Rep variant | biological replicate | percentage "full" capsids | mean |
|---|---|---|---|---|
| AAV6 | R2 | I | 12% | 17% |
| | | II | 18% | |
| | | III | 20% | |
| | R1hc2 | I | 37% | 43% |
| | | II | 45% | |
| | | III | 46% | |
| | R2d1 | I | 20% | 28% |
| | | II | 25% | |
| | | III | 39% | |
| | R8d1c2 | I | 37% | 36% |
| | | II | 38% | |
| | | III | 32% | |
| AAV8 | R2 | I | 18% | 20% |
| | | II | 23% | |
| | | III | 19% | |
| | R8d1c2 | I | 28% | 36% |
| | | II | 47% | |
| | | III | 34% | |
| | R1c2 | I | 41% | 33% |
| | | II | 32% | |
| | | III | 27% | |
| | R8*c2 | I | 62% | 43% |
| | | II | 30% | |
| | | III | 36% | |
| AAV9 | R2 | I | 18% | 18% |
| | | II | 14% | |
| | | III | 22% | |
| | R8d1c2 | I | 36% | 32% |
| | | II | 29% | |
| | | III | 31% | |
| AAVrh.10 | R2 | I | 12% | 17% |
| | | II | 28% | |
| | | III | 11% | |
| | R8d1c2 | I | 27% | 31% |
| | | II | 34% | |
| | | III | 31% | |

590

## *References*


1. **Rittié L, Athanasopoulos T, Calero-Garcia M, Davies ML, Dow DJ, Howe SJ, Morrison A, Ricciardelli I, Saudemont A, Jespers L, Clay TM.** 2019. The Landscape of Early Clinical Gene Therapies outside of Oncology. Mol Ther **27:**1706-1717.
2. **Scott LJ.** 2015. Alipogene tiparvovec: a review of its use in adults with familial lipoprotein lipase deficiency. Drugs **75:**175-182.
3. **Lloyd A, Piglowska N, Ciulla T, Pitluck S, Johnson S, Buessing M, O'Connell T.** 2019. Estimation of impact of RPE65-mediated inherited retinal disease on quality of life and the potential benefits of gene therapy. Br J Ophthalmol doi:10.1136/bjophthalmol-2018-313089.
4. **Waldrop MA, Kolb SJ.** 2019. Current Treatment Options in Neurology-SMA Therapeutics. Curr Treat Options Neurol **21:**25.
5. **Mietzsch M, Penzes JJ, Agbandje-McKenna M.** 2019. Twenty-Five Years of Structural Parvovirology. Viruses **11**.
6. **Srivastava A, Lusby EW, Berns KI.** 1983. Nucleotide sequence and organization of the adeno-associated virus 2 genome. J Virol **45:**555-564.
7. **Bennett A, Mietzsch M, Agbandje-McKenna M.** 2017. Understanding capsid assembly and genome packaging for adeno-associated viruses. Future Virology **12:**283-297.
8. **Weitzman MD, Linden RM.** 2011. Adeno-associated virus biology. Methods Mol Biol **807:**1-23.
9. **Sonntag F, Schmidt K, Kleinschmidt JA.** 2010. A viral assembly factor promotes AAV2 capsid formation in the nucleolus. Proceedings of the National Academy of Sciences of the United States of America **107:**10220-10225.
10. **Ogden PJ, Kelsic ED, Sinai S, Church GM.** 2019. Comprehensive AAV capsid fitness landscape reveals a viral gene and enables machine-guided design. Science **366:**1139-1143.
11. **Gray JT, Zolotukhin S.** 2011. Design and construction of functional AAV vectors. Methods Mol Biol **807:**25-46.
12. **Grieger JC, Samulski RJ.** 2012. Adeno-associated virus vectorology, manufacturing, and clinical applications. Methods Enzymol **507:**229-254.
13. **Qiu J, Soderlund-Venermo M, Young NS.** 2017. Human Parvoviruses. Clin Microbiol Rev **30:**43-113.
14. **Smith RH, Kotin RM.** 1998. The Rep52 gene product of adeno-associated virus is a DNA helicase with 3'-to-5' polarity. J Virol **72:**4874-4881.
15. **Cassell GD, Weitzman MD.** 2004. Characterization of a nuclear localization signal in the C-terminus of the adeno-associated virus Rep68/78 proteins. Virology **327:**206-214.
16. **Im D-S, Muzyczka N.** 1990. The AAV origin-binding protein Rep68 is an ATP-dependent site-specific endonuclease with helicase activity. Cell **61:**447-457.
17. **Di Pasquale G, Stacey SN.** 1998. Adeno-associated virus Rep78 protein interacts with protein kinase A and its homolog PRKX and inhibits CREB-dependent transcriptional activation. J Virol **72:**7916-7925.
18. **King JA, Dubielzig R, Grimm D, Kleinschmidt JA.** 2001. DNA helicase-mediated packaging of adeno-associated virus type 2 genomes into preformed capsids. EMBO J **20:**3282-3291.
19. **Wörner TP, Bennett A, Habka S, Snijder J, Friese O, Powers T, Agbandje-McKenna M, Heck AJR.** 2021. Adeno-associated virus capsid assembly is divergent and stochastic. Nat Commun **12:**1642.
20. **Yoon-Robarts M, Blouin AG, Bleker S, Kleinschmidt JA, Aggarwal AK, Escalante CR, Linden RM.** 2004. Residues within the B' motif are critical for DNA binding by the superfamily 3 helicase Rep40 of adeno-associated virus type 2. J Biol Chem **279:**50472-50481.

21. **Gao G, Vandenberghe LH, Alvira MR, Lu Y, Calcedo R, Zhou X, Wilson JM.** 2004. Clades of Adeno-associated viruses are widely disseminated in human tissues. J Virol **78:**6381-6388.
22. **Grimm D, Kay MA, Kleinschmidt JA.** 2003. Helper virus-free, optically controllable, and two-plasmid-based production of adeno-associated virus vectors of serotypes 1 to 6. Mol Ther **7:**839-850.
23. **Nass SA, Mattingly MA, Woodcock DA, Burnham BL, Ardinger JA, Osmond SE, Frederick AM, Scaria A, Cheng SH, O'Riordan CR.** 2018. Universal Method for the Purification of Recombinant AAV Vectors of Differing Serotypes. Mol Ther Methods Clin Dev **9:**33-46.
24. **Li C, Samulski RJ.** 2020. Engineering adeno-associated virus vectors for gene therapy. Nat Rev Genet **21:**255-272.
25. **Viney L, Bürckstümmer T, Eddington C, Mietzsch M, Choudhry M, Henley T, Agbandje-McKenna M.** 2021. Adeno-associated Virus (AAV) Capsid Chimeras with Enhanced Infectivity Reveal a Core Element in the AAV Genome Critical for both Cell Transduction and Capsid Assembly. J Virol doi:10.1128/jvi.02023-20.
26. **Havlik LP, Simon KE, Smith JK, Klinc KA, Tse LV, Oh DK, Fanous MM, Meganck RM, Mietzsch M, Agbandje-McKenna M, Asokan A.** 2020. Co-evolution of AAV capsid antigenicity and tropism through a structure-guided approach. J Virol doi:10.1128/jvi.00976-20.
27. **Tse LV, Klinc KA, Madigan VJ, Castellanos Rivera RM, Wells LF, Havlik LP, Smith JK, Agbandje-McKenna M, Asokan A.** 2017. Structure-guided evolution of antigenically distinct adeno-associated virus variants for immune evasion. Proc Natl Acad Sci U S A **114:**E4812-e4821.
28. **Xiao X, Li J, Samulski RJ.** 1998. Production of high-titer recombinant adeno-associated virus vectors in the absence of helper adenovirus. J Virol **72:**2224-2232.
29. **Li J, Samulski RJ, Xiao X.** 1997. Role for highly regulated rep gene expression in adeno-associated virus vector production. J Virol **71:**5236-5243.
30. **Farris KD, Pintel DJ.** 2008. Improved splicing of adeno-associated viral (AAV) capsid protein-supplying pre-mRNAs leads to increased recombinant AAV vector production. Hum Gene Ther **19:**1421-1427.
31. **Stutika C, Gogol-Doring A, Botschen L, Mietzsch M, Weger S, Feldkamp M, Chen W, Heilbronn R.** 2015. A Comprehensive RNA Sequencing Analysis of the Adeno-Associated Virus (AAV) Type 2 Transcriptome Reveals Novel AAV Transcripts, Splice Variants, and Derived Proteins. J Virol **90:**1278-1289.
32. **Musayev FN, Zarate-Perez F, Bishop C, Burgner JW, 2nd, Escalante CR.** 2015. Structural Insights into the Assembly of the Adeno-associated Virus Type 2 Rep68 Protein on the Integration Site AAVS1. J Biol Chem **290:**27487-27499.
33. **Pereira DJ, McCarty DM, Muzyczka N.** 1997. The adeno-associated virus (AAV) Rep protein acts as both a repressor and an activator to regulate AAV transcription during a productive infection. J Virol **71:**1079-1088.
34. **Pereira DJ, Muzyczka N.** 1997. The adeno-associated virus type 2 p40 promoter requires a proximal Sp1 interaction and a p19 CArG-like element to facilitate Rep transactivation. J Virol **71:**4300-4309.
35. **Mietzsch M, Smith JK, Yu JC, Banala V, Emmanuel SN, Jose A, Chipman P, Bhattacharya N, McKenna R, Agbandje-McKenna M.** 2020. Characterization of AAV-Specific Affinity Ligands: Consequences for Vector Purification and Development Strategies. Mol Ther Methods Clin Dev **19:**362-373.
36. **Ng R, Govindasamy L, Gurda BL, McKenna R, Kozyreva OG, Samulski RJ, Parent KN, Baker TS, Agbandje-McKenna M.** 2010. Structural characterization of the dual glycan binding adeno-associated virus serotype 6. J Virol **84:**12945-12957.

37. **Im DS, Muzyczka N.** 1989. Factors that bind to adeno-associated virus terminal repeats. J Virol **63:**3095-3104.
38. **Alex M, Weger S, Mietzsch M, Slanina H, Cathomen T, Heilbronn R.** 2012. DNA-binding activity of adeno-associated virus Rep is required for inverted terminal repeat-dependent complex formation with herpes simplex virus ICP8. J Virol **86:**2859-2863.
39. **Ling C, Yin Z, Li J, Zhang D, Aslanidi G, Srivastava A.** 2016. Strategies to generate high-titer, high-potency recombinant AAV3 serotype vectors. Mol Ther Methods Clin Dev **3:**16029.
40. **Wang L, Blouin V, Brument N, Bello-Roufai M, Francois A.** 2011. Production and purification of recombinant adeno-associated vectors. Methods Mol Biol **807:**361-404.
41. **Gao K, Li M, Zhong L, Su Q, Li J, Li S, He R, Zhang Y, Hendricks G, Wang J, Gao G.** 2014. Empty Virions In AAV8 Vector Preparations Reduce Transduction Efficiency And May Cause Total Viral Particle Dose-Limiting Side-Effects. Mol Ther Methods Clin Dev **1:**20139.
42. **Jose A, Mietzsch M, Smith JK, Kurian J, Chipman P, McKenna R, Chiorini J, Agbandje-McKenna M.** 2019. High-Resolution Structural Characterization of a New Adeno-associated Virus Serotype 5 Antibody Epitope toward Engineering Antibody-Resistant Recombinant Gene Delivery Vectors. J Virol **93**.
43. **Wobus CE, Hugle-Dorr B, Girod A, Petersen G, Hallek M, Kleinschmidt JA.** 2000. Monoclonal antibodies against the adeno-associated virus type 2 (AAV-2) capsid: epitope mapping and identification of capsid domains involved in AAV-2-cell interaction and neutralization of AAV-2 infection. J Virol **74:**9281-9293.

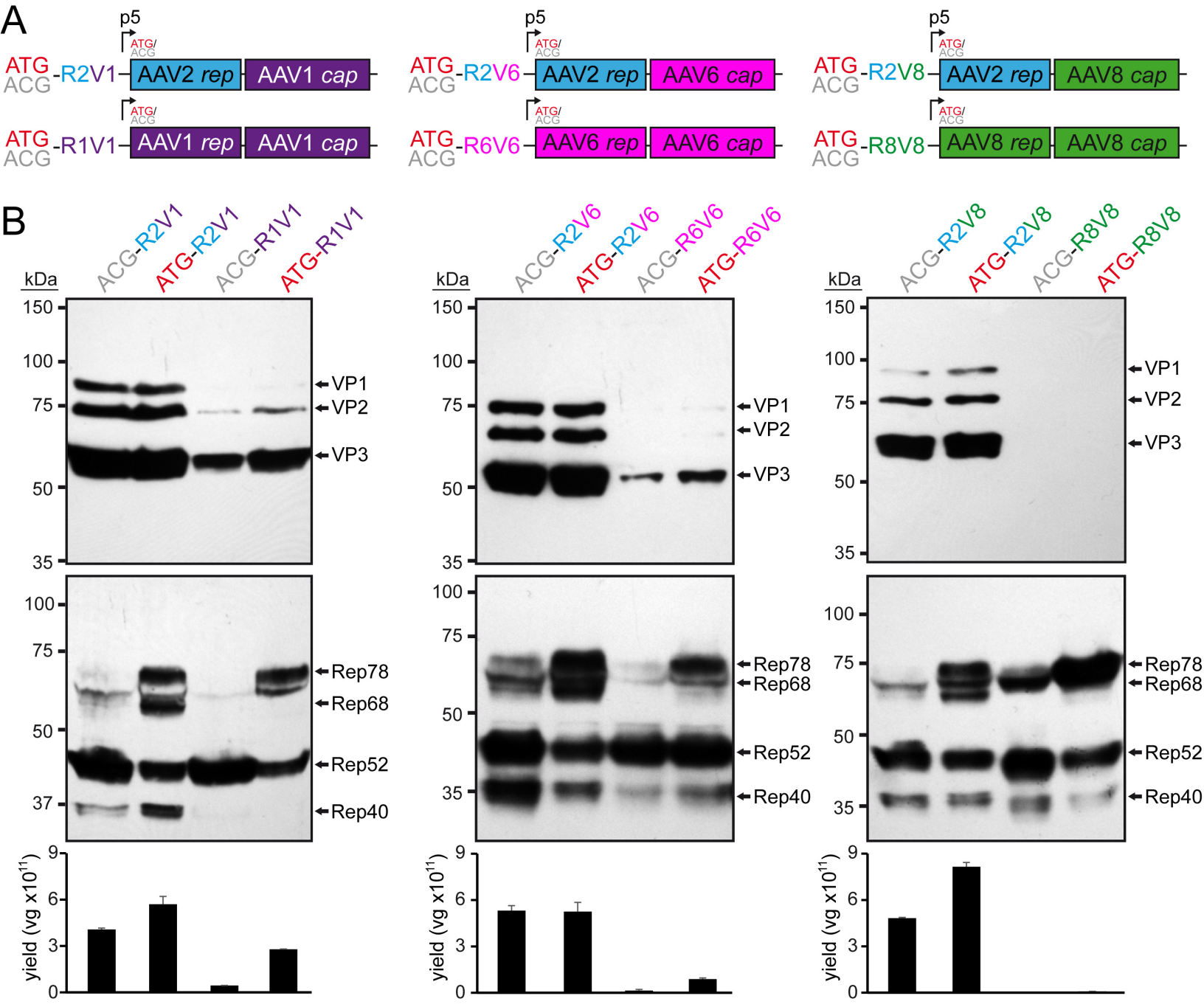

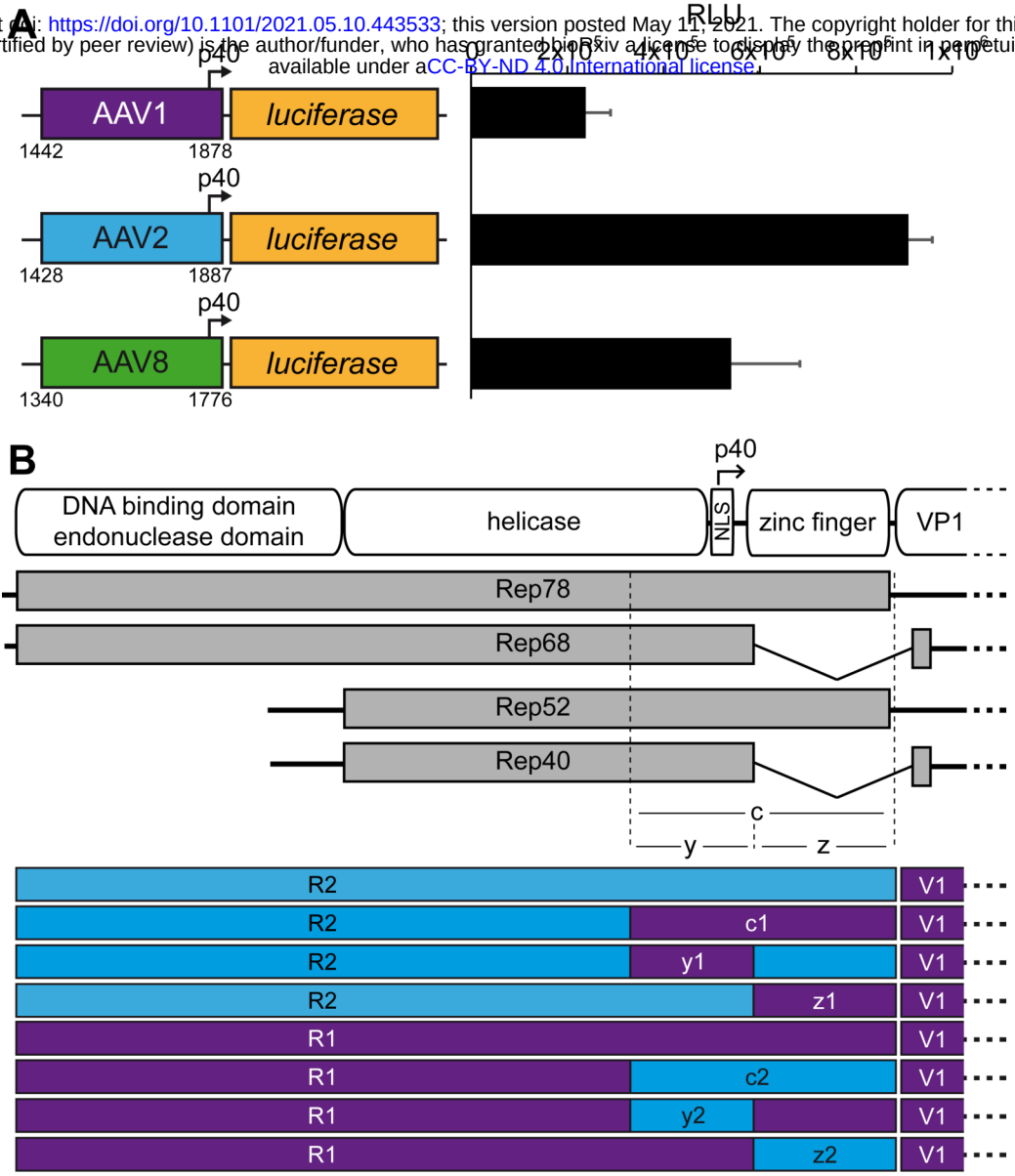


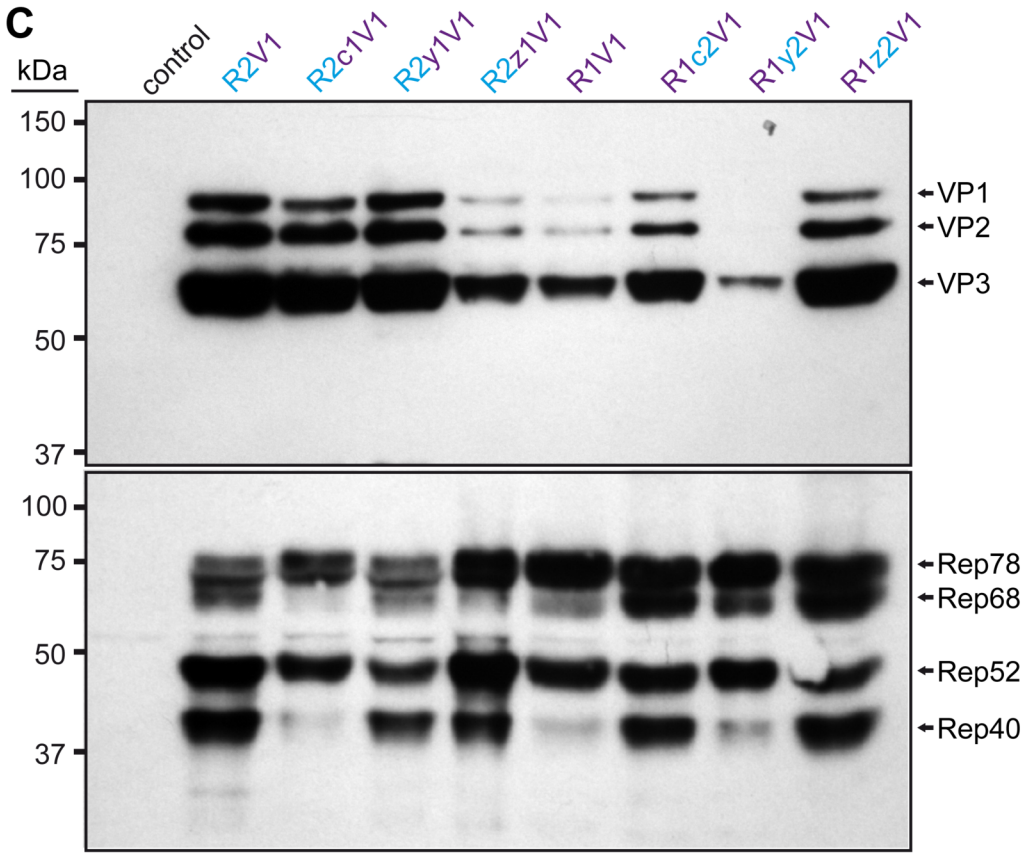

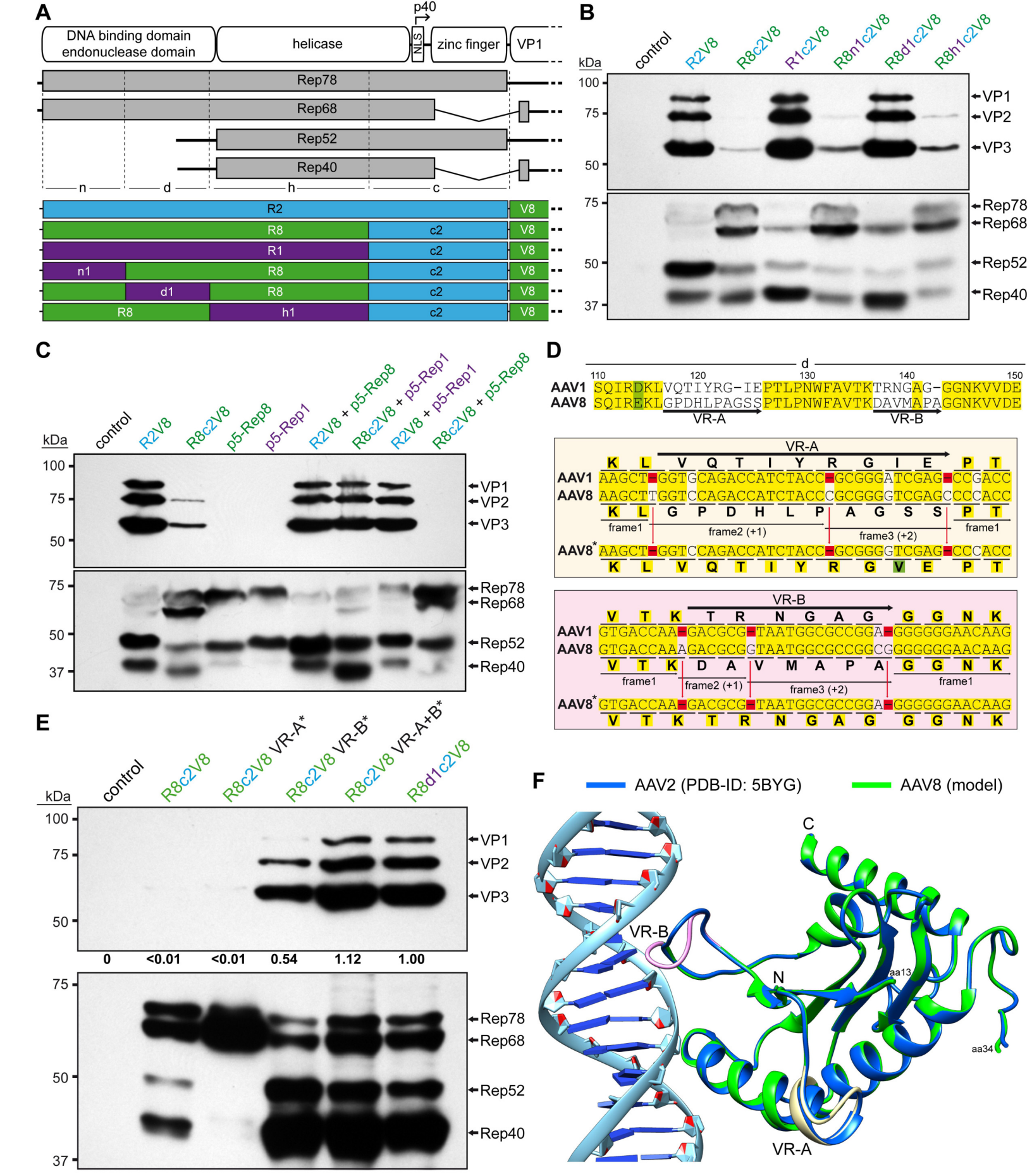
A
p40
DNA binding domain
endonuclease domain
helicase
NLS
zinc finger
VP1
Rep78
Rep68
Rep52
Rep40
n
d
h
c
R2
V8
R8
c2
R1
n1
d1
h1
B
kDa
control
R2V8
R8c2V8
R1c2V8
R8n1c2V8
R8d1c2V8
R8h1c2V8
100
75
50
37
VP1
VP2
VP3
Rep78
Rep68
Rep52
Rep40
C
p5-Rep8
p5-Rep1
R2V8 + p5-Rep8
R8c2V8 + p5-Rep8
R2V8 + p5-Rep1
R8c2V8 + p5-Rep1
D
AAV1 SQIRDKLVQTIYRG-IEPTLPNWFAVTKTRNGAG-GGNKVVDE
AAV8 SQIREKLGPDHLPAGSSPTLPNWFAVTKDAVMAPAGGNKVVDE
VR-A
VR-B
frame1
frame2 (+1)
frame3 (+2)
AAV8*
E
R8c2V8 VR-A*
R8c2V8 VR-B*
R8c2V8 VR-A+B*
R8d1c2V8
0
<0.01
<0.01
0.54
1.12
1.00
F
AAV2 (PDB-ID: 5BYG)
AAV8 (model)
C
N
VR-B
VR-A
aa13
aa34

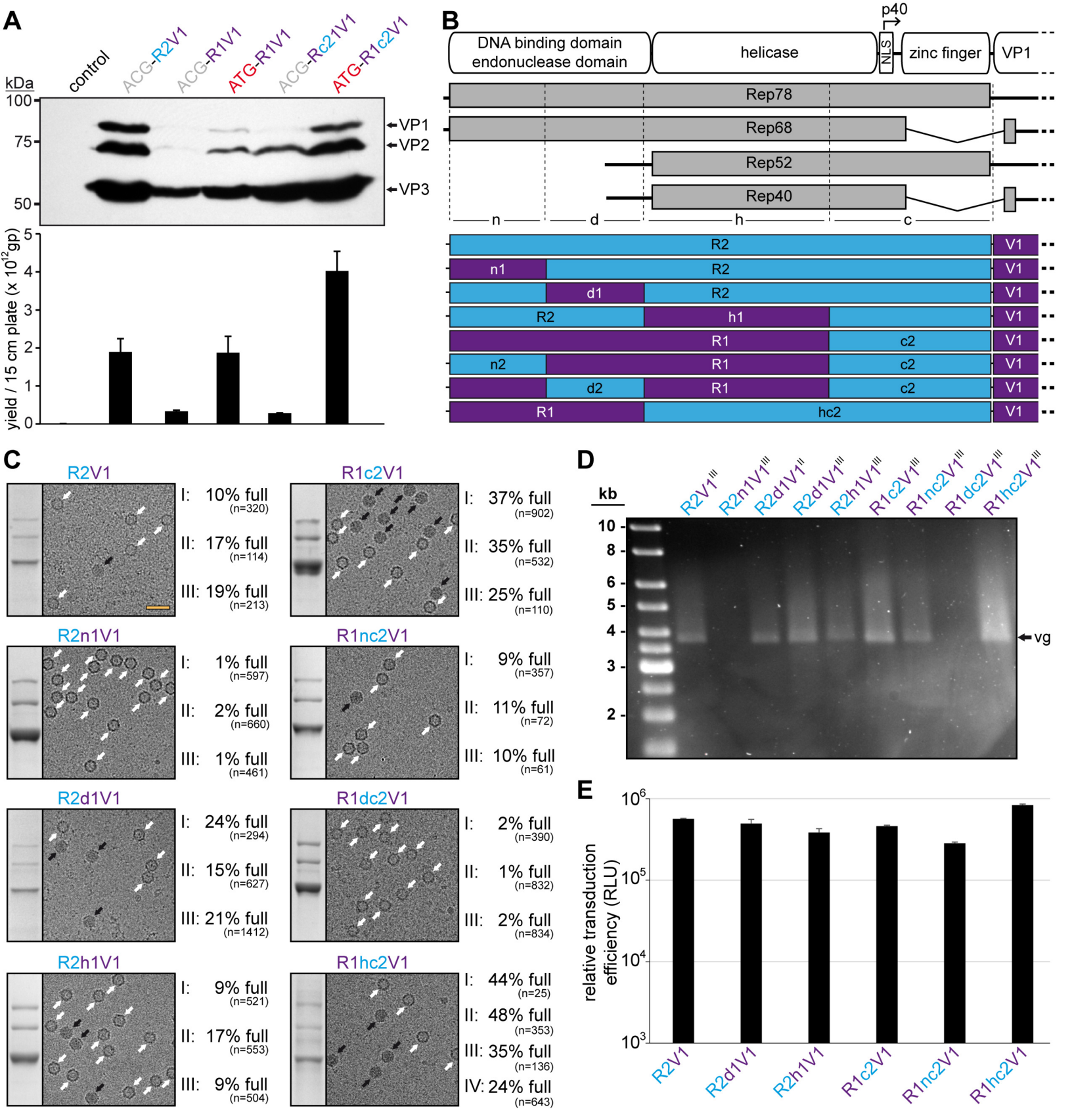

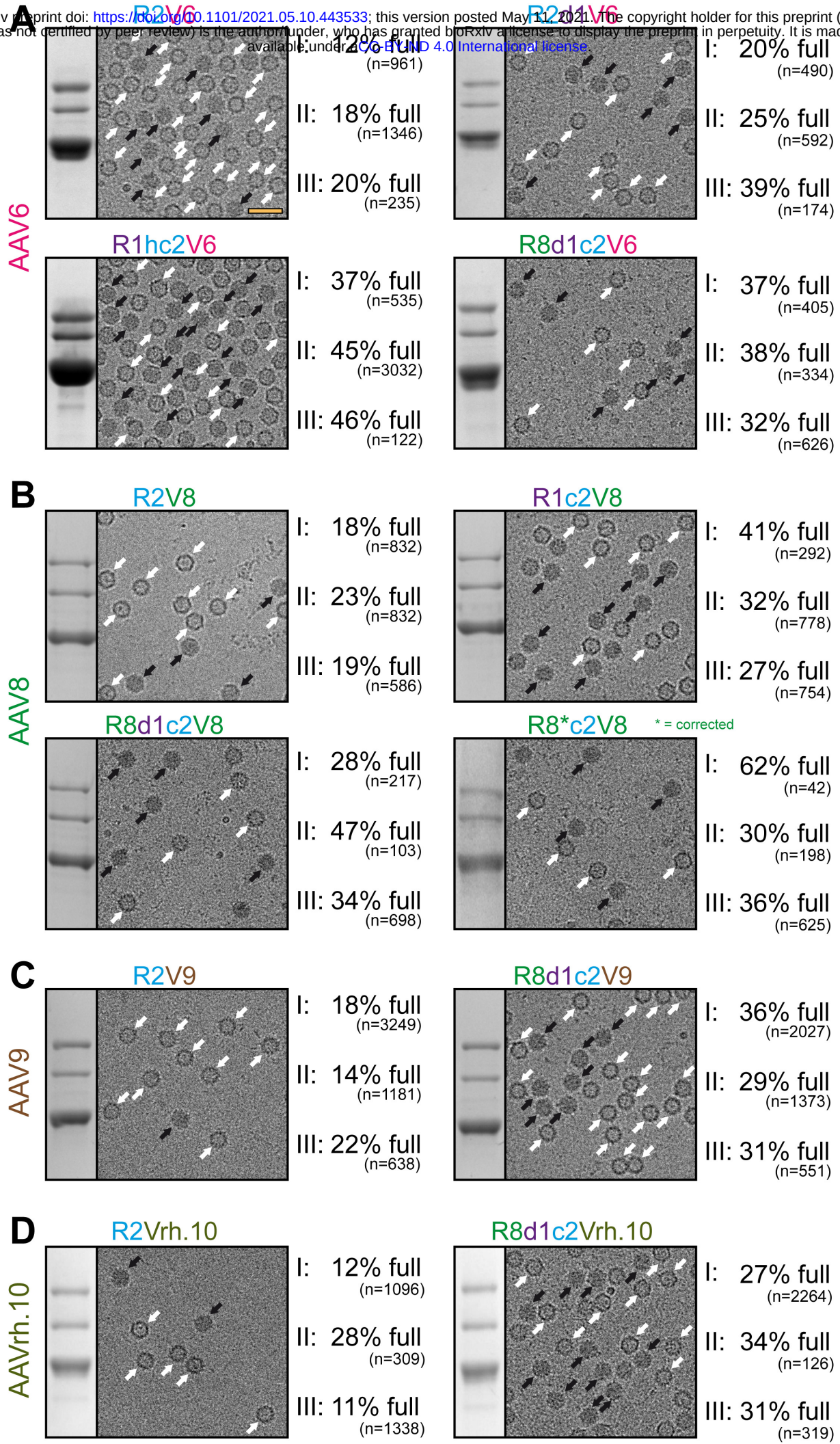

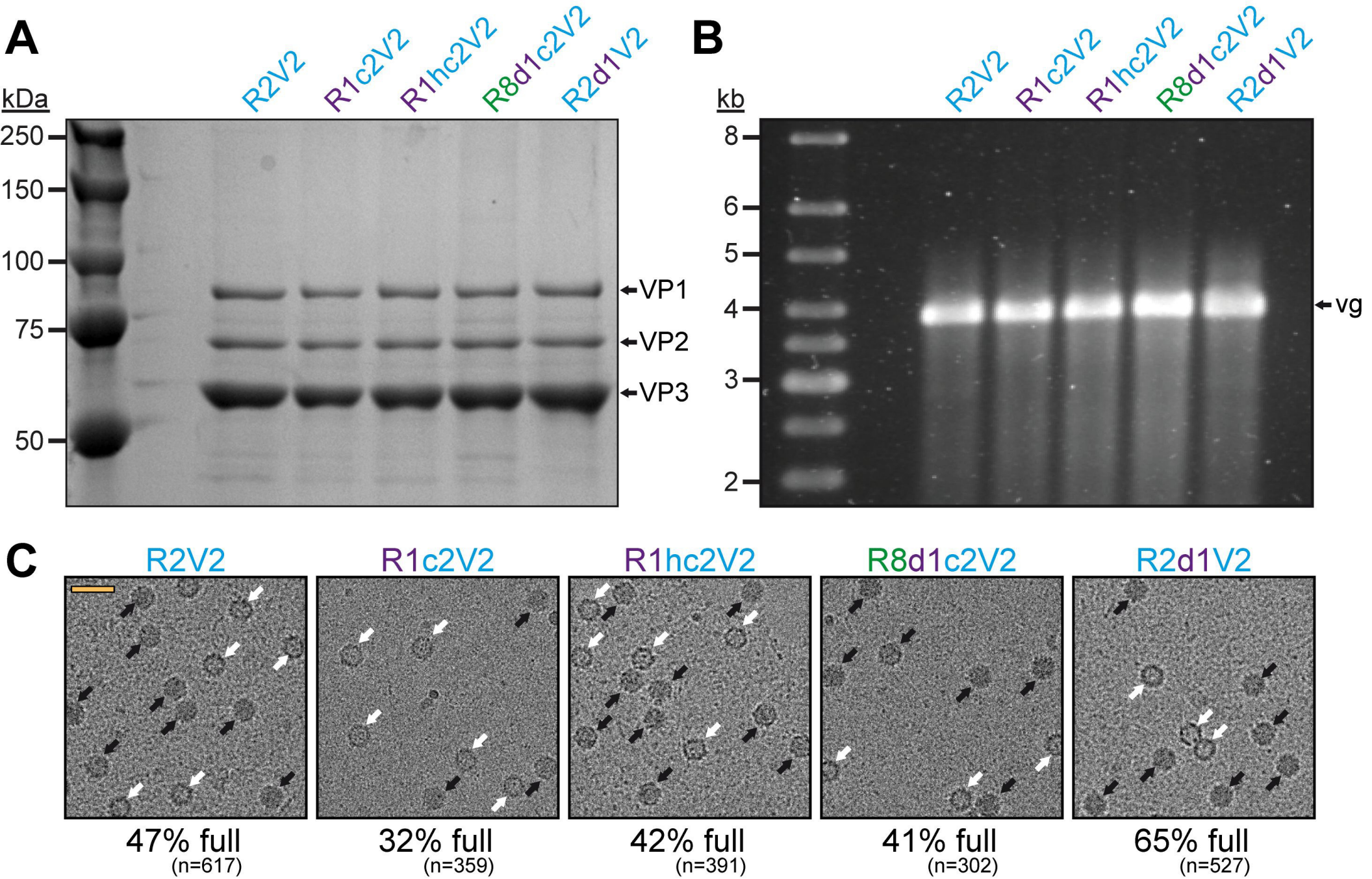
A
kDa
250
150
100
75
50
R2V2
R1c2V2
R1hc2V2
R8d1c2V2
R2d1V2
VP1
VP2
VP3
B
kb
8
6
5
4
3
2
R2V2
R1c2V2
R1hc2V2
R8d1c2V2
R2d1V2
vg
C
R2V2
R1c2V2
R1hc2V2
R8d1c2V2
R2d1V2
47% full
(n=617)
32% full
(n=359)
42% full
(n=391)
41% full
(n=302)
65% full
(n=527)